



## IgG4-Related Ophthalmic Disease with Proptosis

Li-Qiang Zheng<sup>1</sup>, Han-Zhaohui Zheng<sup>2</sup>, Xiang-Chun Han<sup>3</sup>, Xiu-Xiu Mao<sup>1</sup>, Yin-Zhi Zhang<sup>1</sup>

<sup>1</sup>Department of Dermatology, The Hospital of 81<sup>st</sup> Group Army PLA, Zhangjiakou, China

<sup>2</sup>Clinical Medicine Five-year Undergraduate Program, Shanghai Jiao Tong University School of Medicine, Shanghai, China

<sup>3</sup>Department of Pathology, Tianjin Beichen Hospital of Chinese Medicine, Tianjin, China

A 57-year-old Chinese male presented with a 10-year history of significant swelling of bilateral eyes and complained of blurry vision for 3 months. His past medical history was extensive and included hypertension, hypergammaglobulinemia, hyperuricemia, and serum eosinophilia (2008). In addition, in 2008, he was suspected to have pancreatic cancer with liver metastasis; however, he declined treatment due to poor prognosis and an extremely low expected survival rate. In fact, due to limited medical conditions, autoimmune pancreatitis could not be definitively ruled out. Subsequently, in 2012, the patient developed a ureteral stricture, resulting in right renal atrophy and left hydronephrosis accompanied by persistent microscopic hematuria; the ureteral stricture was being treated by placing a left ureteral stent every 3 months. In 2018, the patient experienced a sudden onset of lower abdominal pain. Contrast-enhanced abdominal CT scan revealed aneurysms of the lower abdominal aorta and right common iliac artery, accompanied by thrombosis. He ultimately underwent interventional treatment with arterial stent placement. His family history was unremarkable.

Laboratory tests revealed markedly elevated total IgE (1964.0 KU/L; reference range: 0-60 KU/L) and increased IgG levels (53.18 g/L; reference range: 7-17 g/L). Further analysis of the IgG subclasses revealed markedly elevated serum IgG4 (38,058 mg/L; reference range: 36-2,090 mg/L), IgG1 (17,312 mg/L; reference range: 3,941-10,444 mg/L), and IgG3 (1,170 mg/L; reference range: 101-895 mg/L). The complete blood count indicated eosinophilia (2.31; reference range: 0.02-0.50 x 10<sup>9</sup>/L) and markedly elevated erythrocyte sedimentation rate (52 mm/h; reference range: 0-15 mm/h). All other test parameters were within normal limits. Notably, the results did not support the presence of necrotizing myopathy, Rosai-Dorfman disease, ANCA-associated vasculitides, sarcoidosis, thyroid disease, or infection. The publication of this study has obtained written informed consent from the patient's daughter.

Physical examination revealed diffuse bilateral swelling of the orbital tissues and eyelids (Figure 1a). Fundus examination showed bilateral optic nerve atrophy (Figure 1b). Magnetic resonance imaging of the brain/orbits revealed severe proptosis of both globes, along with diffuse and significant thickening of the bilateral periorbital skin, subcutaneous tissue, and retrobulbar tissue. The bilateral extraocular muscles and lacrimal glands were diffusely enlarged, leading to compression of the optic nerves (Figure 1c). Contrast-enhanced abdominal computed tomography revealed abdominal aortic aneurysm and a right common iliac aneurysm following stent surgery; right renal atrophy following left renal pelvis and ureteral stent surgery (Figure 1d); and multiple low-density lesions in the liver, along with a non-enhancing area in the pancreatic tail (Figure 1e). Microscopic examination of lacrimal gland tissues revealed a prominent infiltration of lymphoplasmacytes and eosinophils (Figure 1f). Immunohistochemistry revealed an elevated IgG4:IgG ratio of approximately 70%, meeting the histopathological criteria for IgG4-related ophthalmic disease (ROD).

IgG4-ROD is a clinical entity histologically characterized by abundant IgG4-positive plasma cells, storiform fibrosis, obstructive phlebitis, and eosinophil infiltration, often accompanied by peripheral eosinophilia and, in most cases, elevated serum IgG4 levels.<sup>1,2</sup> In addition, a previous report described some patients with atopic disease, elevated serum gammaglobulin levels, and hypocomplementemia.<sup>3</sup>

The disorder primarily affects middle-aged men and is rarely seen in children.<sup>4</sup> It can affect organs across multiple systems, either synchronously or metachronously, including the salivary glands, pancreas, biliary tree, lymph nodes, kidneys, lungs, retroperitoneum, aorta, eye, and skin. In 2015, Goto et al.<sup>5</sup> established a diagnostic triad for IgG4-ROD in the proposed ophthalmic diagnostic criteria.



**Corresponding author:** Li-Qiang Zheng, Department of Dermatology, The Hospital of 81<sup>st</sup> Group Army PLA, Zhangjiakou, China

**e-mail:** zlqiang1976@163.com



**Received:** May 15, 2025 **Accepted:** June 12, 2025 **Available Online Date:** 31.10.2025 • **DOI:** 10.4274/balkanmedj.galenos.2025.2025-5-34

Available at [www.balkanmedicaljournal.org](http://www.balkanmedicaljournal.org)

**ORCID iDs of the authors:** L.Q.Z. 0000-0002-7482-8578; H.Z.Z. 0009-0003-3268-3889; X.C.H. 0000-0001-6747-3628; X.X.M. 0000-0003-3711-0214; Y.Z.Z. 0009-0006-6990-3218.

**Cite this article as:** Zheng LQ, Zheng HZ, Han XC, Mao XX, Zhang YZ. IgG4-Related Ophthalmic Disease with Proptosis. Balkan Med J; 2025; 42(6):557-9.

Copyright@Author(s) - Available online at [http://balkanmedicaljournal.org/](http://balkanmedicaljournal.org)

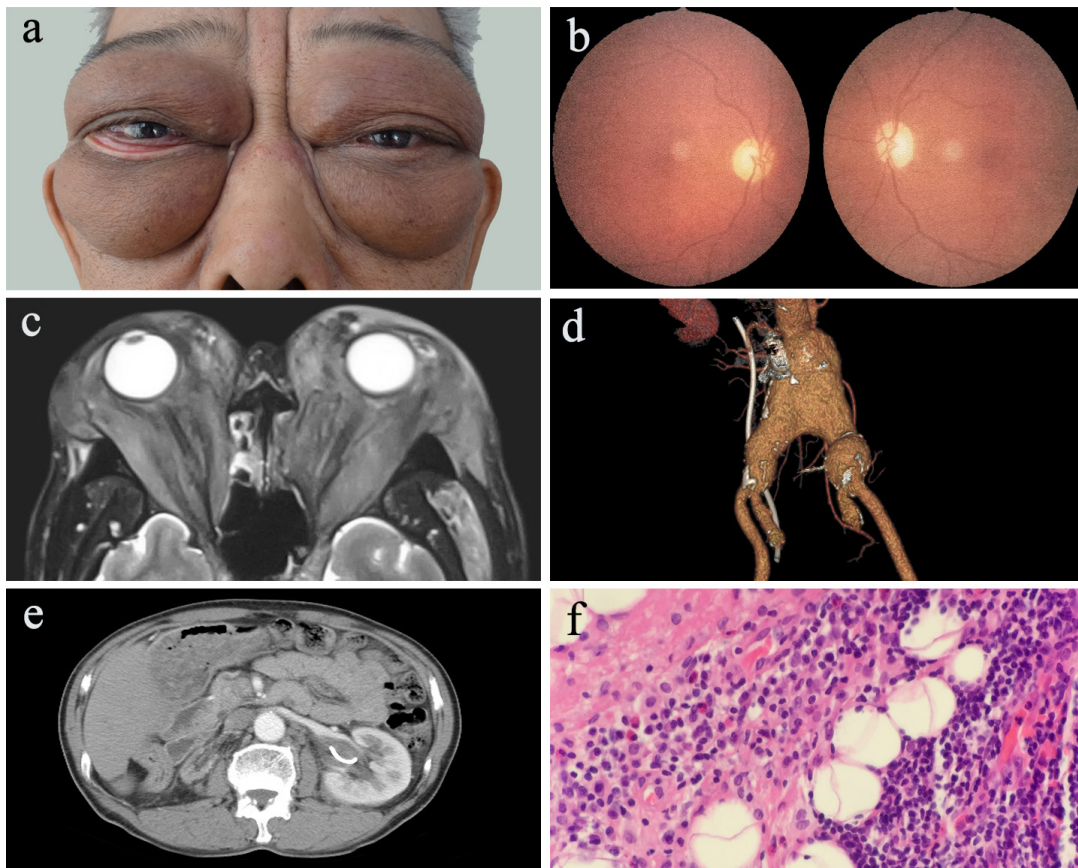


**FIG. 1.** (a) Diffuse bilateral periorbital swelling and proptosis. (b) Bilateral optic nerve atrophy. (c) MRI of the brain/orbits findings. (d-e) Enhanced Abdominal CT results. (f) Microscopy examination of lacrimal gland tissues (H&E  $\times 200$ ).  
*MRI*, magnetic resonance imaging; *CT*, computed tomography.

Moreover, bilateral involvement in IgG4-ROD is clearly associated with extraophthalmic manifestations of IgG4-ROD.<sup>6</sup>

Histopathologically, it often exhibits varying degrees of storiform fibrosis, the severity of which depends on the specific organ involved. One report indicated that the storiform fibrosis is characteristic of autoimmune pancreatitis; however, dense fibrosis is not typically observed in Mikulicz disease or skin IgG4-ROD.<sup>7</sup> Imaging studies, in particular, play a crucial role in the diagnostic process.

Early clinical manifestations are often non-specific and can easily lead to misdiagnosis. As mentioned above, formal histopathological examination of any accessible lesion remains the gold standard for diagnosing IgG4-ROD. Clinically, if the diagnosis can be confirmed through biopsy of a more accessible peripheral site, biopsy of pancreatic lesions should be avoided. However, in the initial phases of our case, due to the difficulty in obtaining biopsies from the pancreatic lesion, making differentiation from pancreatic cancer was extremely challenging.

Corticosteroids are the mainstay of treatment and typically elicit an excellent response; however, relapse is common upon discontinuation or tapering of corticosteroid therapy.<sup>8</sup> A higher post-treatment serum IgG4 concentration has been associated with

an increased risk of disease recurrence. Similarly, individuals with IgG4-ROD have an increased risk of relapse if their baseline serum IgE levels are elevated. In addition, baseline IgE levels at the time of diagnosis may serve as a predictor of the disease trajectory.<sup>9</sup> Notably, the combination of rituximab with palpebral surgery has shown promising results in patients with IgG4-ROD presenting with orbital pseudotumors.<sup>10</sup> Due to financial constraints, the patient was unable to undergo treatment with rituximab and other biologics.

In this case, the patient's clinical condition showed moderate improvement following the initiation of oral corticosteroid induction therapy. However, in June 2024, he experienced a ruptured abdominal aortic aneurysm and ultimately declined further interventional treatment. Unfortunately, the patient passed away 2 months later.

**Informed Consent:** The publication of this study has obtained written informed consent from the patient's daughter.

**Authorship Contributions:** Concept- L.Q.Z.; Design- L.Q.Z.; Supervision- H.Z.Z.; Materials- X.C.H.; Data Collection and/or Processing- L.Q.Z., H.Z.Z.; Analysis and/or Interpretation- H.Z.Z., X.C.H.; Literature Review- X.C.H.; Writing- H.Z.Z., X.X.M., Y.Z.Z.; Critical Review- L.Q.Z., X.X.M., Y.Z.Z.

**Conflict of Interest:** No conflict of interest was declared by the authors.

## REFERENCES

1. Stone JH, Zen Y, Deshpande V. IgG4-related disease. *N Engl J Med.* 2012;366:539-551. [\[CrossRef\]](#)
2. Deshpande V, Zen Y, Chan JK, et al. Consensus statement on the pathology of IgG4-related disease. *Mod Pathol.* 2012;25:1181-1192. [\[CrossRef\]](#)
3. Kubo K, Yamamoto K. IgG4-related disease. *Int J Rheum Dis.* 2016;19:747-762. [\[CrossRef\]](#)
4. Umebara H, Okazaki K, Masaki Y, et al. Comprehensive diagnostic criteria for IgG4-related disease (IgG4-RD). 2011. *Mod Rheumatol.* 2012;22:21-30. [\[CrossRef\]](#)
5. Goto H, Takahira M, Azumi A; Japanese study group for IgG4-related ophthalmic disease. Diagnostic criteria for IgG4-related ophthalmic disease. *Jpn J Ophthalmol.* 2015;59:1-7. [\[CrossRef\]](#)
6. Wu A, Andrew NH, McNab AA, Selva D. Bilateral IgG4-related ophthalmic disease: a strong indication for systemic imaging. *Br J Ophthalmol.* 2016;100:1409-1411. [\[CrossRef\]](#)
7. Katerji R, Smoller BR. Immunoglobulin-G4-related skin disease. *Clin Dermatol.* 2021;39:283-290. [\[CrossRef\]](#)
8. Zhou J, Peng Y, Peng L, et al. Serum IgE in the clinical features and disease outcomes of IgG4-related disease: a large retrospective cohort study. *Arthritis Res Ther.* 2020;22:255. [\[CrossRef\]](#)
9. Culver EL, Sadler R, Bateman AC, et al. Increases in IgE, eosinophils, and mast cells can be used in diagnosis and to predict relapse of IgG4-related disease. *Clin Gastroenterol Hepatol.* 2017;15:1444-[\[CrossRef\]](#)
10. Aouidad I, Schneider P, Zmuda M, Gottlieb J, Viguer M. IgG4-related disease with orbital pseudotumors treated with rituximab combined with palpebral surgery. *JAMA Dermatol.* 2017;153:355-356. [\[CrossRef\]](#)